Bone Marrow Mesenchymal Stem Cell-derived Exosomes Exert Therapeutic Effects by Attenuating Fibrosis and Facilitating Hepatocyte Proliferation via the Anti-pyroptosis Pathway in a Rat Cirrhosis Model

Yichi Zhang
Second Affiliated Hospital of Harbin Medical University
Xinsheng Nie
xinjiang shengchan jianshe bingtuan: Xinjiang Production and Construction Corps
Lijuan Wang
xinjiang shengchan jianshe bingtuan: Xinjiang Production and Construction Corps
Zhuzhi Wan
xinjiang shengchan jianshe bingtuan: Xinjiang Production and Construction Corps
Hao Jin
xinjiang shengchan jianshe bingtuan: Xinjiang Production and Construction Corps
Ronghui Pu
xinjiang shengchan jianshe bingtuan: Xinjiang Production and Construction Corps
Meihui Liang
xinjiang shengchan jianshe bingtuan: Xinjiang Production and Construction Corps
Yuan Chang
Second Affiliated Hospital of Harbin Medical University
Yang Gao
Second Affiliated Hospital of Harbin Medical University
Hailong Zhang
xinjiang shengchan jianshe bingtuan: Xinjiang Production and Construction Corps
Shizhu Jin (drshizhujin@hrbmu.edu.cn)
Second Affiliated Hospital of Harbin Medical University https://orcid.org/0000-0003-3613-0926

Research

Keywords: Exosomes, BMMSCs, Liver cirrhosis, Pyroptosis

Posted Date: September 22nd, 2021

DOI: https://doi.org/10.21203/rs.3.rs-907834/v1

Bone marrow mesenchymal stem cell-derived exosomes exert therapeutic effects by attenuating fibrosis and facilitating hepatocyte proliferation via the anti-pyroptosis pathway in a rat cirrhosis model

Zhang YC[1], Nie XS[2], Wang LJ[2], Wan ZZ[2], Jin H[2], Pu RH[2], Liang MH[2], Chang Y[1], Gao Y[1], Zhang HL[2], Jin SZ[1,2*].

[1] Department of Gastroenterology and Hepatology, The Second Affiliated Hospital, Harbin Medical University, Harbin, Heilongjiang Province, China.

[2] The Xinjiang Production and Construction Corps Tenth Division Beitun Hospital, Beitun, Xinjiang Province, China.

[*] Corresponding author. Correspondence and requests for materials should be addressed to Shizhu Jin. (email: drshizhujin@hrbmu.edu.cn)

Abstracts

Background: Liver cirrhosis, which lacks a specific therapy, induces a substantial economic burden and affects quality of life. Exosomes are nanosized vesicles that are secreted by cells transfer bioactive molecules to regulate metastasis and have attracted immense interest as a therapeutic option for liver cirrhosis. Therefore, in this study, we explored the efficacy and dose of exosomes derived from rat bone marrow mesenchymal stem cells (Exos-rBMMSC) in a hepatic cirrhosis rat model.

Results: Four weeks after exosome therapy, NLRP3, GSDMD, cleaved caspase-1, IL-1β and IL-18 expression levels in the 200 μg and 400 μg Exos-rBMMSC groups were significantly decreased compared to those in the liver cirrhosis group ($P<0.05$). Similar results were observed in the hepatic function assay; serum levels of aspartate aminotransferase and alanine aminotransferase were decreased, and albumin was increased. The histopathology results showed that 200 μg and 400 μg of Exos-rBMMSC significantly relieved collagen deposition, while 100 μg of Exos-rBMMSC induced no marked improvements compared to those in the liver cirrhosis group. The localization of PKH67-labelled Exos-rBMMSC was verified microscopically, and these particles coexpressed PCNA, NLRP3, GSDMD and Caspase-1.

Conclusions: Our findings suggest that Exos-rBMMSC accelerate hepatocyte proliferation and relieve liver fibrosis, which may be a promising therapeutic strategy for liver cirrhosis.

Key words: Exosomes; BMMSCs; Liver cirrhosis; Pyroptosis

Introduction

Liver cirrhosis is the terminal phase of all types of chronic hepatic diseases. Currently, without an effective therapy for liver cirrhosis, patients are more likely to experience hospital readmissions, hepatocellular carcinoma and death, which results in a substantial economic burden. The annual death rate of liver cirrhosis worldwide is as high as 1.32 million [1]. Therefore, developing an effective therapy is an urgent problem to be solved.

In recent years, accumulating evidence from preclinical experiments and clinical trials has demonstrated that rat bone marrow mesenchymal stem cell (rBMMSC) transplantation can alleviate collagen accumulation and improve liver function [2, 3]. However, the therapeutic effect is limited by low differentiation efficiency, and most stem cells are obstructed in the pulmonary vasculature [4]. Moreover, the clinical application of stem cell transplantation is hampered by complications such as tumorigenicity and immunologic rejection [5]. Hence, exosomes (Exos), which possess similar biological topology as stem cells, are important paracrine mediators and have become a promising and advanced cell-free remedy. Exos are vesicles that are 30~150 nm in diameter, are secreted by all kinds of cells, and transfer functional mircoRNAs (miRNAs), mRNAs, proteins and cytokines, and these vesicles have inspired substantial research enthusiasm for mediating intercellular metastasis [6; 7]. However, few studies have focused on the applicable doses of Exos, which is a gap that hampers practical clinical applications.

In this study, we aimed to explore the optimal dose of Exos derived from rBMMSCs (Exos-rBMMSC) for treating liver cirrhosis. The therapeutic effects of 100 μg, 200 μg and 400 μg of Exos-rBMMSC were evaluated by examining pyroptosis inhibition, pathological histology, liver function and molecular biology in vivo and in vitro. In addition, the distribution of Exos was examined by near-infrared fluorescence (NIRF) imaging. Overall, our results suggested that Exos-BMMSC alleviated liver cirrhosis and enhanced hepatic function.

Results

Liver cirrhosis model establishment.

Rat liver cirrhosis models were verified by analysing specimens, and the results showed that the surface of the model liver was grainy and pale, and the organ was smaller in size than the control liver (Fig. 1A). Haematoxylin and eosin (HE)-stained cirrhotic liver sections showed cellular necrosis, inflammatory cell infiltration and pseudolobuli formation compared to those in the control group (Fig. 1B & 1D). Masson staining of sections showed that compared to those in the control group, hepatic collagen production and collagen deposition were obviously present (Fig. 1C & 1E).

rBMMSCs alleviated hepatocyte pyroptosis.

We confirmed that pyroptosis-related proteins were highly expressed in the liver cirrhosis model (Fig. 1F). In addition, 4 weeks of rBMMSC transplantation via caudal vein injection significantly alleviated the degree of liver fibrosis (Fig. 1G & 1H) and markedly restrained the expression of pyroptosis-related proteins (NLRP3, GSDMD and cleaved caspase-1, Fig. 1I-1M, $^{*}P<0.05$). IL-1β and IL-18, which are pyroptosis-related inflammatory factors, were decreased after 4 weeks of rBMMSC transplantation (Fig. 1N & 1O, $^{**}P<0.01$).

Paracrine effect of rBMMSCs on inhibiting hepatocyte pyroptosis.

After hepatocytes and rBMMSCs were cocultured for 24 h, PKH67 dye was observed in hepatocytes, which indicated that rBMMSCs affected hepatocytes in a paracrine manner (Fig. 2A-2D). GW4869 (dissolved in DMSO, 10 μM) is an inhibitor of membrane neutral sphingomyelin, which participates in Exo generation and release[8]. To assess the effect of Exos-rBMMSC on hepatocytes, the following groups were established: control group (untreated hepatocytes), CCl_4 group (hepatocytes were treated with 10 mM CCl_4 (dissolved in DMSO)), CCl_4+DMSO group (hepatocytes were treated with CCl_4 (10 mM) and 1% DMSO), CCl_4+GW4869 group (hepatocytes were treated with CCl_4 (10 mM) and GW4869 (10 μM)), CCl_4+CCS group (hepatocytes were treated with CCl_4 (10 mM) and rBMMSC cell culture supernatant (CCS)), and CCl_4+CCS+GW4869 group (hepatocytes were

treated with CCl_4 (10 mM), GW4869 (10 μM) and rBMMSC CCS). Pyroptosis-related protein (NLRP3, GSDMD, cleaved caspase-1 and IL-1β) expression levels in the CCl_4+CCS group were significantly decreased (Fig. 2E-2I, $^{*}P<0.05$ *vs.* the CCl_4 group). Importantly, the expression of NLRP3, GSDMD, cleaved caspase-1 and IL-1β in the CCl_4+CCS group was significantly decreased compared to the expression in the CCl_4+CCS+GW4869 group, suggesting the attenuating effects of Exos-rBMMSC on hepatocyte pyroptosis. In addition, IL-1β and IL-18 expression levels in the CCl_4+CCS group were dramatically decreased (Fig. 2K-2L, $^{****}P<0.0001$ *vs.* the CCl_4 group). Besides, the cell counting kit-8 (CCK-8) results showed that the viability of cells in the CCl_4+CCS group was significantly higher than that in the other groups (Fig. 2J, $^{\#\#}P<0.01$).

Exos-rBMMSCs alleviated hepatocyte pyroptosis in vitro.

Exos-rBMMSC were isolated by differential ultracentrifugation, as shown in Fig. 3A. The morphology of Exos-rBMMSC was examined by transmission electron microscopy (TEM) and showed a saucer-like shape (Fig. 3B). The concentration of Exos-rBMMSC was 1.0×10^{10} particles/ml, and 98% of the particles ranged from 30 nm to 200 nm (Fig. 3C). Exo-specific markers were highly expressed in Exos-rBMMSC (Fig. 3D). Based on these results, we successfully purified Exos-rBMMSC. PKH67-labelled Exos-rBMMSC were internalized by hepatocytes, as shown in Fig. 3E and 3F. Exos-rBMMSC dramatically promoted CCl_4-induced hepatocyte proliferation, as shown by EdU assays (Fig. 3G-3J, $^{****}P<0.0001$ *vs.* the CCl_4 group). Similar results were obtained from the CCK-8 assay, and the cell viability of the Exo group was significantly higher than that of the CCl_4 group (Fig. 3K, $^{***}P<0.001$). Additionally, compared to that in the CCl_4 group, IL-1β and IL-18 expression in the Exo group was significantly lower (Fig. 3L-3M, $^{***}P<0.001$). In contrast to those in the CCl_4 group, the expression levels of pyroptosis-related proteins in the Exo group were notably decreased (Fig. 3N-3R, $^{*}P<0.05$).

The distribution of Exos-rBMMSC in vivo.

DiR-labelled Exos-rBMMSC were injected through the tail vein. At 0, 3 and 24 h postinjection, the fluorescence intensities in major organs, including the heart, lung,

liver, spleen and kidney, were measured by an in vivo imaging system. At 3 h postinjection, Exos-rBMMSC were mainly concentrated in the liver and spleen. At 24 h postinjection, Exos-rBMMSC migrated to the lung, liver and spleen (Fig. 4A). To further confirm whether PKH67-labelled Exos-rBMMSC were taken up by injured hepatocytes, an immunofluorescence assay was performed. The colocalization of PKH67-labelled Exos-rBMMSC with NLRP3, GSDMD and caspase-1 is shown in Fig. 4B.

Exos-rBMMSC reduced pyroptosis protein expression in vivo.

To determine the optimal dose of Exos-rBMMSC, 100 μg, 200 μg and 400 μg of Exos-rBMMSC were injected via the tail vein. Four weeks postinjection, liver samples from the different groups were collected. Compared to that in the CCl_4 group, the expression level of NLRP3 in the 200 μg and 400 μg Exos-rBMMSC groups was significantly decreased, while that in the 100 μg Exos-rBMMSC group was not significantly different (Fig. 4D, $^{**}P<0.01$). NLRP3 expression in the 200 μg Exos-rBMMSC group was significantly lower than that in the 100 μg Exos-rBMMSC group and higher than that in the 400 μg Exos-rBMMSC group (Fig. 4D, $^{\#}P<0.05$). Similar results were observed for GSDMD, caspase-1 and IL-1β loci. These proteins were expressed at significantly higher levels in the CCl_4 group than in the other groups (Fig. 4D-4G, $^{**}P<0.01$). The expression of these proteins in the 200 μg Exos-rBMMSC group was dramatically lower than that in the 100 μg Exos-rBMMSC group but higher than that in the 400 μg Exos-rBMMSC group (Fig. 4D-4G, $^{\#}P<0.05$). In addition, serum IL-1β and IL-18 levels showed similar results (Fig. 4H-4I).

Exos-rBMMSC further ameliorated histopathological changes.

HE-stained liver sections from the hepatic cirrhosis group showed inflammatory cell infiltration, collagen deposition and pseudolobule formation (Fig. 5A2). Four weeks postinjection, the Exos-rBMMSC-treated groups showed pathological remission (Fig. 5A3-5A5). Masson-stained sections showed that 4 weeks of treatment with 200 μg and 400 μg of Exos-rBMMSC significantly relieved collagen deposition, while 100 μg of Exos-rBMMSC induced no marked improvements compared to the liver cirrhosis group (Fig. 5B, $^{**}P<0.01$). Similar results were observed in the

semiquantitative collagen analysis; 200 μg and 400 μg of Exos-rBMMSC induced dramatic reductions in collagen levels compared to those in the liver cirrhosis group (Fig. 5K, $P<0.01$). There were no significant differences between the 100 μg Exos-rBMMSC and liver cirrhosis groups (Fig. 5K, $P>0.05$).

Exos-rBMMSC inhibited hepatocyte pyroptosis and accelerated proliferation.

Immunohistochemical assays showed that NLRP3, GSDMD and caspase-1 were more highly expressed in the liver cirrhosis group than in the other groups, and the levels in the 200 μg and 400 μg Exos-rBMMSC groups were dramatically decreased (Fig. 5C-5E). Notably, proliferating cell nuclear antigen (PCNA), which is the basic element in DNA replication and repair, was significantly increased in the 200 μg and 400 μg Exos-rBMMSC groups compared to the liver cirrhosis group (Fig. 5F & 5J, $^{****}P<0.0001$). Quantitative analysis showed that NLRP3-positive cells in the 400 μg Exos-rBMMSC group were significantly reduced compared to those in the liver cirrhosis group (Fig. 5G, $^{****}P<0.0001$) but were not significantly different compared to those in the 100 μg and 200 μg Exos-rBMMSC groups (Fig. 5G, $P>0.05$). Compared with those in the cirrhosis group, GSDMD-positive cells in the Exos-rBMMSC groups were dramatically decreased (Fig. 5H, $^{***}P<0.001$). GSDMD-positive cells in the 400 μg Exos-rBMMSC group were markedly decreased compared to those in the 200 μg and 100 μg Exos-rBMMSC groups (Fig. 5H, $^{\#\#\#\#}P<0.0001$). Similar results were observed in the number of caspase-1-positive cells (Fig. 5I).

Exos-rBMMSC enhanced liver function.

Liver function was assessed by measuring aspartate aminotransferase (AST) and alanine aminotransferase (ALT) and albumin (ALB) expression levels. Compared to those in the 200 μg and 400 μg Exos-rBMMSC groups, AST and ALT expression levels in the liver cirrhosis group were markedly increased; in contrast, ALB was markedly decreased (Fig. 5L-5N, $^{*}P<0.05$). AST and ALT expression in the 200 μg Exos-rBMMSC group was significant higher than that in the 400 μg Exos-rBMMSC group, while there were no difference compared to that in the 100 μg Exos-rBMMSC group (Fig. 5L-5M, $^{\#}P<0.05$). ALB expression in the 200 μg Exos-rBMMSC group

was markedly higher than that in the 100 μg Exos-rBMMSC group and dramatically lower than that in the 400 μg Exos-rBMMSC group (Fig. 5N, $^{\#}P<0.05$).

Discussion

Liver cirrhosis is the end stage of all types of hepatic diseases, and the complications cause a substantial economic burden and affect quality of life. For treating liver cirrhosis and its complications, searching for effective therapies and exploring the pathogenesis of liver cirrhosis have been hot topics in recent years. In this study, we demonstrated that Exos-rBMMSC promoted hepatocyte proliferation and alleviated liver fibrosis by restraining hepatocyte pyroptosis.

Pyroptosis is characterized by membrane pore formation, cytolysis and the release of proinflammatory cytokines, including IL-1β, IL-18 and HMGB1 [9]. Previous studies showed that hepatocyte pyroptosis and the release of inflammasome components induced hepatic stellate cell (HSC) activation and liver fibrosis [10; 11]. Consistent with these findings, our study showed that pyroptosis-related proteins, including NLRP3, caspase-1, GSDMD, cleaved caspase-1 and IL-1β, were markedly upregulated in cirrhotic liver tissues. Additionally, we confirmed that 4 weeks of rBMMSC treatment by caudal vein injection significantly downregulated these proteins. To further investigate the mechanism by which rBMMSCs affect hepatocytes, a coculture system of rBMMSCs and hepatocytes was established, and the results indicated that the effects were mediated by a paracrine pathway.

Exos serve as central mediators of intercellular communication owing to their unique nucleic acids and proteins, which drive their utilization as cell-free therapeutics [12]. Accumulating evidence has demonstrated that Exos derived from stem cells alleviate liver fibrosis. The transplantation of Exos from human umbilical cord-MSCs (Exos-hucMSC) mitigated liver fibrosis by reducing liver inflammation, collagen deposition and epithelial-to-mesenchymal transition (EMT) [13]. Exos-rBMMSC could reduce oxidative stress and accelerate liver regeneration in a liver injury model [14]. Additionally, Exos-rBMMSC showed suppressive effects by reducing liver necrotic areas and enhancing anti-inflammatory cytokines [15]. A recent study demonstrated that Exos-rBMMSC restrained liver fibrosis by inhibiting HSC activation through the Wnt/β-catenin pathway [16]. Exos produced by miR-181-5p-overexpressing adipose-derived mesenchymal stem cells (ADSCs)

significantly inhibited collagen I, vimentin, α-SMA and fibronectin expression [17]. Similar research showed that circ-0000623-overexpressing ADSCs attenuated liver fibrosis by activating hepatocyte autophagy [18]. However, the optimal dose of Exos-rBMMSC for use in liver cirrhosis therapy has not been discussed. In this study, we explored the therapeutic dose of Exos-rBMMSC for liver cirrhosis. It is worth mentioning that the effect of Exos on the rat traumatic brain injury (TBI) model was dose-dependent in a 7-day therapeutic window. Exos (200 μg and 100 μg per rat) significantly alleviated long-term neuroinflammation in a TBI model, while 200 μg Exos did not provide further therapeutic effects [19]. Another study reported that extracellular nanovesicles (EVs) from 1×10^8 ADSCs had better attenuating effects on liver fibrosis than EVs from 1×10^6 and 1×10^7 ADSCs [20]. According to our results, injection of both 200 μg and 400 μg of Exos-rBMMSCs via the tail vein significantly restrained hepatocyte pyroptosis and collagen deposition. Interestingly, our results showed that 400 μg of Exos-rBMMSC showed a better therapeutic effect than 200 μg of Exos-rBMMSC. The present study was the first to suggest the optimal dose of Exos-rBMMSCs for liver cirrhosis, laying an experimental foundation for clinical applications. Further studies are warranted to discover the molecules within Exos-rBMMSC, such as DNA, mRNA, noncoding RNA and specific growth factors, that promote hepatocyte proliferation, restrain pyroptosis, and reduce collagen deposition.

Conclusions

Overall, in this study, we demonstrated that Exos-rBMMSC significantly accelerated hepatocyte proliferation and relieved liver fibrosis, and the effect may depend on restraining hepatocyte pyroptosis. More importantly, the effect of Exos-rBMMSC on hepatocytes was dose-dependent, and 400 μg of Exos-rBMMSC may be the optimal dose for treating liver cirrhosis. Our findings provide experimental data and supporting theories for clinical applications.

Methods

Establishment of the rat liver cirrhosis model

Sprague-Dawley rats (130~150 g, male) were obtained from the animal facility of the Second Affiliated Hospital of Harbin Medical University. A liver cirrhosis model was established as we described previously [3]. Briefly, 50% CCl_4 (dissolved in oil) was intraperitoneally injected twice each week for 4 weeks. After 4 weeks of stimulation, the animals were examined by histopathology. In addition, all experiments and methods were approved by the Experimental Centre of the Second Affiliated Hospital of Harbin Medical University.

Cell culture

The purification and identification of rBMMSCs were described in our previous study [3]. rBMMSCs were cultured in DMEM/F12 medium (Sigma, USA), 10% FBS (35-081-cv, Corning, USA), and 1% penicillin-streptomycin (pH = 7.4, Sigma, USA). Exos-rBMMSC were collected from third-passage rBMMSCs to fifth-passage rBMMSCs. BRL rat hepatocytes were purchased from BEINA Biology Company and cultured in MEM (Sigma, USA) and 10% FBS.

Purification and characterization of Exos-rBMMSC

rBMMSC culture supernatant was collected after the cells were cultured in Exo-free medium (DMEM/F12-Sigma, 10% Exo-free FBS, 1% penicillin-streptomycin) for 24 h. Then, Exos were purified according to the protocol in the Journal of Extracellular Vesicles [21, 22]. Briefly, the supernatant was concentrated by differential ultracentrifugation, followed by centrifugation at 300 ×g for 10 min, 2000 ×g for 10 min, and 10,000 ×g for 30 min. Finally, the supernatant was ultracentrifuged at 100,000 ×g for 70 min twice. The precipitate was resuspended in 200 μl of phosphate-buffered saline (PBS). The protein concentration of Exos-rBMMSCs was measured by a BCA assay [23]. To characterize the purified vesicles as Exos, the morphology was examined by TEM, and the diameters were measured and analysed by a Zeta View Particle Metrix (Zeta View PMX 110). The exosomal protein markers CD9, TSG101, and TSG70 (1:1000, Abcam) and negative marker calnexin (1:1000, Abcam) were examined by western blotting.

PKH67 staining

According to the protocol and the published study [24], to prepare the 2× dye solution, 2 μl of PKH67 ethanolic dye was added to 1 ml of Diluent C. Then, 1 ml of the Exos solution was rapidly added into the 2× dye solution and mixed slowly for 4 min. To suspend redundant staining, 2 ml of serum-free FBS was added. PBS was added to adjust the volume to 14 ml, and the mixture was centrifuged at 100,000 × g at 4 °C for 90 min. The supernatant was removed, and PKH67-labelled Exos were resuspended in 200 μl of PBS. Similarly, rBMMSCs were stained with PKH67 according to the Exo procedure.

Coculture of hepatocytes and rBMMSC

The Transwell coculture system (3450, Corning Costar) consisted of 1×10^6 hepatocytes and 1×10^6 rBMMSCs. Hepatocytes were seeded in 6-well plates, and PKH67-labelled rBMMSCs were cultured in the Transwell inserts. After 24 h of coculture, the hepatocytes were observed under a fluorescence microscope (Zeiss-DMI8).

Exo uptake assessment

PKH67-labelled Exos-rBMMSC (100 μg) were added to hepatocytes and cultured in 6-well plates with FBS-free medium. After 24 h of incubation, the hepatocytes were assessed by fluorescence microscopy.

Cell viability analysis

The viability of untreated hepatocytes, hepatocytes treated with CCl_4 (10 mM) and PBS, and hepatocytes treated with CCl_4 (10 mM) and 100 μg Exos was assessed by CCK-8 (APExBIO-K1018) and 5-ethynyl-2′-deoxyuridine (EdU) imaging kits (UE, China). Briefly, 5×10^3 hepatocytes were seeded in 96-well plates for 24 h (n = 15). Then, CCl_4 (10 mM) was added to 10 plates, and the same volume of PBS was added to 5 plates. After 12 h of incubation, the medium was replaced with MEM+100 μg Exos or MEM+PBS. Cell viability was measured according to the manufacturer's protocol after 4 hours of culture.

Biodistribution of Exos-rBMMSC

To detect the distribution of the Exos-rBMMSC in vivo, Exos-rBMMSC were

stained with 1,1'-dioctadecyl-3,3,3',3'-tetramethylindotricarbocyanine iodide (DiR, D12731, Invitrogen, Life Technologies), which was obtained commercially from Sigma. DiR-stained Exos (100 μg) were injected into CCl_4-induced rats. At 0, 3 and 24 h after tail vein injection, ex vivo fluorescent images of different organs, including the heart, lung, liver, spleen and kidney, were taken by an in vivo imaging system (Night OWL II LB983).

Immunofluorescence and immunohistochemical assays

Immunofluorescence and immunohistochemical examinations were conducted as described previously [3]. Briefly, frozen liver sections (4 μm) were used for immunofluorescence assays, and paraffin liver sections (4 μm) were used for immunohistochemical assays. Primary antibodies against NLRP3 (1:50, NOVUS), GSDMD (1:1000, Abcam), Caspase-1 (1:200, Sigma), and PCNA (1:200, Affinity) were added and incubated overnight at 4 ℃. Then, immunofluorescence images were taken by fluorescence microscopy (Zeiss-DMI8), and immunohistochemical images were obtained by an Olympus (BX41) microscope and semiquantitatively measured by Fiji software.

Western blotting

The western blot procedure was described in our previous study [3]. Briefly, proteins were extracted from frozen liver tissue. After electrophoresis, the proteins were transferred to nitrocellulose membranes, which were incubated with β-actin (1:1000, Abcam), NLRP3 (1:5000, NOVUS), GSDMD (1:1000, Abcam), cleaved caspase-1 (1:1000, CST), and IL-1β (1:1000, Abclonal) antibodies overnight at 4 °C. Then, the nitrocellulose membranes were incubated with HRP-conjugated secondary antibodies (1:5000, Boster). Finally, images were taken using the ImageQuant LAS 4000 mini machine (GE).

ELISA

Rat tissue and serum samples were obtained after euthanasia. Fresh frozen hepatic tissues were homogenized with PBS at 4 °C according to the manufacturer's protocol. After centrifugation at 120,000 g at 4 °C for 20 min, the supernatant was collected. Liver function was evaluated by measuring the levels of ALT, AST and

ALB with ELISA kits (Nanjing Jiancheng, China). The IL-1β and IL-18 levels in serum and cell supernatants were examined by ELISA kits (Boster, China) according to the protocol.

Histopathological assays

The liver tissues were fixed with 4% paraformaldehyde and embedded in paraffin. Liver sections (4 μm) were stained with HE to observe pathological morphology and with Masson to examine collagen deposition. Semiquantitative analysis was performed by Fiji software.

Statistical analyses

GraphPad Prism 9 software (Version 9.0.1, Inc.) was used to analyse the data by one-way analysis of variance (ANOVA). All data are displayed as the mean ± standard deviation. Statistical significance was defined as $P<0.05$. All figures were prepared by GraphPad Prism 9 and Photoshop 7.1.

Reference

1. Asrani SK, Devarbhavi H, Eaton J, Kamath PS. Burden of liver diseases in the world. J Hepatol. 2019;70(1):151-171.
2. Luo XY, Meng XJ, Cao DC, Wang W, Zhou K, Li L, et al. Transplantation of bone marrow mesenchymal stromal cells attenuates liver fibrosis in mice by regulating macrophage subtypes. Stem Cell Res Ther. 2019;10(1):16.
3. Zhang YC, Li RN, Rong WW, Han MZ, Cui CH, Feng ZN, et al. Therapeutic effect of hepatocyte growth factor-overexpressing bone marrow-derived mesenchymal stem cells on CCl_4-induced hepatocirrhosis. Cell Death Dis. 2018;9(12):1186.
4. de Witte SFH, Luk F, Sierra Parraga JM, Gargesha M, Merino A, Korevaar SS, et al. Immunomodulation By Therapeutic Mesenchymal Stromal Cells (MSC) Is Triggered Through Phagocytosis of MSC By Monocytic Cells. Stem Cells. 2018;36(4):602-615.
5. Lee AS, Tang C, Rao MS, Weissman IL, Wu JC. Tumorigenicity as a clinical hurdle for pluripotent stem cell therapies. Nat Med. 2013;19(8):998-1004.
6. Jeppesen DK, Fenix AM, Franklin JL, Higginbotham JN, Zhang Q, Zimmerman LJ, et al. Reassessment of Exosome Composition. Cell. 2019;177(2):428-445.
7. Kalluri R, LeBleu VS. The biology, function, and biomedical applications of exosomes. Science. 2020;367(6478):eaau6977.
8. Mariadelva Catalano, Lorraine O'Driscoll. Inhibiting extracellular vesicles formation and release: a review of EV inhibitors. J Extracell Vesicles. 2019;9(1):1703244.
9. Wang YP, Gao WQ, Shi XY, Ding JJ, Liu W, He HB, et al. Chemotherapy drugs induce pyroptosis through caspase-3 cleavage of a gasdermin. Nature. 2017;547(7661):99-103.
10. Gaul S, Leszczynska A, Alegre F, Kaufmann B, Johnson CD, Adams LA, et al. Hepatocyte pyroptosis and release of inflammasome particles induce stellate cell activation and liver fibrosis. J Hepatol. 2021;74(1):156-167.
11. Wree A, Eguchi A, McGeough MD, Pena CA, Johnson CD, Canbay A, et al.

NLRP3 inflammasome activation results in hepatocyte pyroptosis, liver inflammation, and fibrosis in mice. Hepatology. 2014;59(3):898-910.

12. Ha DH, Kim HK, Lee J, Kwon HH, Park GH, Yang SH, et al. Mesenchymal stem/stromal cell-derived Exosomes for immunomodulatory therapeutics and skin regeneration. Cells. 2020;9(5):1157.
13. Li T, Yan Y, Wang B, Qian H, Zhang X, Shen L, et al. Exosomes derived from human umbilical cord mesenchymal stem cells alleviate liver fibrosis. Stem Cells Dev. 2013;22(6):845-54.
14. Damania A, Jaiman D, Teotia AK, Kumar A. Mesenchymal stromal cell-derived exosome-rich fractionated secretome confers a hepatoprotective effect in liver injury. Stem Cell Res Ther. 2018;9(1):31.
15. Tamura R, Uemoto S, Tabata Y. Immunosuppressive effect of mesenchymal stem cell-derived exosomes on a concanavalin A-induced liver injury model. Inflamm Regen. 2016;36:26.
16. Rong X, Liu J, Yao X, Jiang T, Wang Y, Xie F. Human bone marrow mesenchymal stem cells-derived exosomes alleviate liver fibrosis through the Wnt/β-catenin pathway. Stem Cell Res Ther. 2019;10(1):98.
17. Qu Y, Zhang Q, Cai X, Li F, Ma Z, Xu M, et al. Exosomes derived from miR-181-5p-modified adipose-derived mesenchymal stem cells prevent liver fibrosis via autophagy activation. J Cell Mol Med. 2017;21(10):2491-2502.
18. Zhu M, Liu X, Li W, Wang L. Exosomes derived from mmu-circ-0000623-modified ADSCs prevent liver fibrosis via activating autophagy. Hum Exp Toxicol. 2020;39(12):1619-1627.
19. Zhang Y, Zhang Y, Chopp M, Zhang ZG, Mahmood A, Xiong Y. Mesenchymal Stem Cell-Derived Exosomes Improve Functional Recovery in Rats After Traumatic Brain Injury: A Dose-Response and Therapeutic Window Study. Neurorehabil Neural Repair. 2020;34(7):616-626.
20. Han HS, Lee H, You D, Nguyen VQ, Song DG, Oh BH, Shin S, Choi JS, Kim JD, Pan CH, Jo DG, Cho YW, Choi KY, Park JH. Human adipose stem cell-derived extracellular nanovesicles for treatment of chronic liver fibrosis. J Control

Release. 2020;320:328-336.

21. Clayton A, Boilard E, Buzas EI, Cheng L, Falcón-Perez JM, Gardiner C, et al. Considerations towards a roadmap for collection, handling and storage of blood extracellular vesicles. J Extracell Vesicles. 2019;8(1):1647027.
22. Clotilde Théry, Sebastian Amigorena, Graça Raposo, Aled Clayton. Isolation and characterization of exosomes from cell culture supernatants and biological fluids. Curr Protoc Cell Biol. 2006;Chapter 3:Unit 3.22.
23. Xu F, Zhong JY, Lin X, Shan SK, Guo B, Zheng MH, et al. Melatonin alleviates vascular calcification and ageing through exosomal miR-204/miR-211 cluster in a paracrine manner. J Pineal Res. 2020;68(3):e12631.
24. Liu JT, Zhu LH, Wang LH, Chen YJ, Giri BR, Li JJ, et al. Isolation and Characterization of Extracellular Vesicles from Adult Schistosoma japonicum. J Vis Exp. 2018;(135):57514.

Figure legends

Figure 1. The alleviation of pyroptosis by rBMMSCs in the context of liver cirrhosis. Specimens of the control and cirrhotic liver models are shown in Fig. 1A. Pathological HE- and Masson-stained sections of control and cirrhotic liver tissues are shown (Fig. 1B-1E). Pyroptosis-related proteins were highly expressed in the liver cirrhosis model (Fig. 1F). Pathological sections showed significant alleviation in the rBMMSC transplantation group (Fig. 1G-1H). Pyroptosis-related proteins in the BMMSC group were significantly downregulated compared to those in the liver cirrhosis group (Fig. 1I-1M, $^{*}P<0.05$ *vs.* the CCl_4 group). IL-1β and IL-18 expression in the BMMSC group was dramatically decreased (Fig. 1N-1O, $^{**}P<0.01$ *vs.* the CCl_4 group). The data are displayed as the means ± SD.

Figure 2. Paracrine effect by which rBMMSCs inhibit hepatocyte pyroptosis. PKH67 dye was transferred to hepatocytes by rBMMSCs via the paracrine pathway (Fig. 2A-2D). Pyroptosis-related proteins in the CCl_4+CCS group were significantly decreased compared to those in the CCl_4 group and CCl_4+CCS+GW4869 group (Fig. 2E-2I, $^{**}P<0.01$). The expression of pyroptosis-related proteins in the CCl_4+DMSO and CCl_4+GW4869 groups was not significantly different compared to that in the CCl_4 group (Fig. 2E-2I). Cell viability in the CCl_4+CCS group was significantly higher than that in the other groups (Fig. 2J, $^{\#\#}P<0.01$). The expression of IL-1β and IL-18 in the CCl_4+CCS group was dramatically lower than that in the other treatment groups (Fig. 2K-2L, $^{**}P<0.01$). The data are displayed as the means ± SD.

Figure 3. Effects of Exos-rBMMSC on CCl_4-induced hepatocytes. The extraction protocol of Exos-rBMMSCs is shown (Fig. 3A). TEM morphology and nanoparticle tracking analysis (NTA) results are shown (Fig. 3B-3C). HSP70, TSG101, CD9 and calnexin expression in the rBMMSC and Exos-rBMMSC groups is shown (Fig. 3D). PKH67-labelled Exos-rBMMSC were internalized by hepatocytes, as observed under a fluorescence microscope (Fig. 3E-3F). Hepatocyte proliferation in the CCl_4 group was dramatically increased (Fig. 3G-3K, $^{***}P<0.001$ *vs.* the CCl_4 group). IL-1β and IL-18 expression in the Exo group was significantly decreased (Fig. 3L-3M, $^{***}P<0.001$ *vs.* the CCl_4 group). NLRP3, GSDMD, cleaved caspase-1 and IL-1β

458 expression in the Exo group was significantly decreased compared to that in the CCl_4
459 group (Fig. 3N-3R, $^{*}P<0.05$). The data are displayed as the means ± SD.
460 **Figure 4. Distribution of Exos-rBMMSC and the therapeutic effect on liver**
461 **cirrhosis.** The distribution of Exos-rBMMSCs was examined by NIRF at 0 h, 3 h and
462 24 h postinjection. At 3 h postinjection, Exos-rBMMSC were mainly concentrated in
463 the liver and were mainly concentrated in the liver and lung at 24 h postinjection (Fig.
464 4A). The colocalization of NLRP3, GSDMD and caspase-1 with PKH67 dye are
465 shown in Fig. 4B. Compared to that in the CCl_4 group, NLRP3, GSDMD, cleaved
466 caspase-1, and IL-1β expression in the 200 μg and 400 μg Exos-rBMMSC groups was
467 dramatically decreased (Fig. 4C-4G, $^{**}P<0.01$). The expression of NLRP3 in the 100
468 μg Exos-rBMMSC group was not significantly different compared to that in the CCl_4
469 group (Fig. 4D, $P>0.05$). The expression of GSDMD, cleaved caspase-1 and IL-1β in
470 the 100 μg Exos-rBMMSC group was dramatically decreased compare to that in the
471 CCl_4 group (Fig. 4E-4G, $^{**}P<0.01$). The expression of NLRP3, GSDMD, cleaved
472 caspase-1 and IL-1β in the 200 μg Exos-rBMMSC group was significantly higher
473 than that in the 400 μg Exos-rBMMSC group (Fig. 4C-4G, $^{\#}P<0.05$). IL-1β and IL-18
474 expression in the 200 μg and 400 μg Exos-rBMMSC groups were dramatically lower
475 than that in the CCl_4 group (Fig. 4H-4I, $^{\#\#}P<0.001$), while the expression in the 100
476 μg Exos-rBMMSC group was not different from that in the CCl_4 group (Fig. 4H-4I,
477 $P>0.05$). IL-1β and IL-18 expression in the 200 μg Exos-rBMMSC group were
478 significantly lower than that in the 100 μg Exos-rBMMSC group but was higher than
479 that in the 400 μg Exos-rBMMSC group (Fig. 4H-4I, $^{\#\#}P<0.01$). The data are
480 displayed as the means ± SD.
481 **Figure 5. The therapeutic effect of Exos-BMMSC on liver cirrhosis was assessed**
482 **in pathological sections and by measuring liver function.** HE-stained sections from
483 the control, liver cirrhosis and Exos-rBMMSC-treated groups are shown (Fig. 5A).
484 Masson-stained sections from the different treatment groups are shown (Fig. 5B).
485 Semiquantitative analysis of the collagen-positive area showed that the areas in the
486 200 μg and 400 μg Exos-rBMMSC groups were significantly decreased compared
487 with those in the liver cirrhosis group (Fig. 5K, $^{**}P<0.01$). The collagen area in the

200 μg Exos-rBMMSC group was significantly lower than that in the 100 μg Exos-rBMMSC group but was higher than that in the 400 μg Exos-rBMMSC group (Fig. 5K, $^{\#}P<0.05$). NLRP3-, GSDMD-, caspase-1- and PCNA-positive cells were assessed by immunohistochemistry (Fig. 5C-5F). Semiquantitative analysis showed that NLRP3-, GSDMD-, caspase-1- and PCNA-positive cells in the 100 μg, 200 μg and 400 μg Exos-rBMMSC groups were significantly lower than those in the liver cirrhosis group (Fig. 5G-5J, $^{**}P<0.01$). The numbers of GSDMD-, caspase-1- and PCNA-positive cells in the 200 μg Exos-rBMMSC group were dramatically lower than those in the 100 μg Exos-rBMMSC group but were higher than those in the 400 μg Exos-rBMMSC group (Fig. 5G-5J, $^{\#}P<0.05$). NLRP3-positive cells in the 200 μg Exos-rBMMSC group were not significantly different from those in the 100 μg and 400 μg Exos-rBMMSC groups (Fig. 5G). AST and ALT expression in the 200 μg and 400 μg Exos-rBMMSC groups was significantly decreased, but ALB expression was significantly increased compared to that in the liver cirrhosis group (Fig. 5L-5N, $^{*}P<0.05$). The expression of AST and ALT in the 400 μg Exos-rBMMSC group was dramatically lower, while the expression of ALB was higher than that in the 200 μg Exos-rBMMSC group (5L-5N, $^{\#}P<0.05$). The data are displayed as the means ± SD.

Abbreviations

Exos: Exosomes; rBMMSC: rat bone marrow mesenchymal stem cells; Exos-rBMMSC: Exosomes derived from rat bone marrow mesenchymal stem cell; CCS: cell culture supernatant; EVs: Extracellular nanovesicles; miRNAs: mirco-RNA; Exos-hucMSC: Exos from human umbilical cord-MSCs; NIRF: Near-infrared fluorescence; HE: Hematoxylin and Eosin; ADSCs:Adipose-derived mesenchymal stem cells; EMT: Epithelial-to-mesenchymal transition; TBI: Traumatic brain injury; TEM: Transmission electronic microscopy; CCK8: Cytotoxicity kit-8; EdU: 5-Ethynyl-2′-deoxyuridine; AST: aspartate aminotransferase; DiR: 1,1'-Dioctadecyl-3,3,3',3'-tetramethylindotricarbocyanine iodide; ALT: alanine aminotransferase; ALB: albumin; ANOVA: One-way analysis of variance.

Authors' contributions

Zhang YC designed and completed experiments. Jin SZ and Nie XS involved in experiment design. Zhang YC, Nie XS and Wang LJ contributed to paper writing. Jin H, Pu RH and Liang MH contributed to data analysis. Chang Y, Gao Y and Zhang HL involved in drawing scientific pictures. All authors read and approved the final manuscript.

Funding

This research was supported by grant from the Xinjiang Production and Construction Corps [2020AB020]. The funders had no role in study design, data collection and analysis, decision to publish, or preparation of the manuscript.

Availability of data and materials

All data generated or analysed during this study are included in this published article.

Consent for publication

All authors agree to be published.

Competing interests

All authors declare no conflicts of interest in this work.

Ethics approval and consent to participate

We confirmed all experiments and methods performed in this study in

accordance with the 2000 Helsinki Declaration and were approved by the Experimental Center of the Second Affiliated Hospital of Harbin Medical University.

Acknowledgements

We thanks the scientific research center of the Second Affiliated Hospital of Harbin Medical University for technical guidance. We also appreciated the support of the Experimental Animal Center of the Second Affiliated Hospital of Harbin Medical University.

Figures

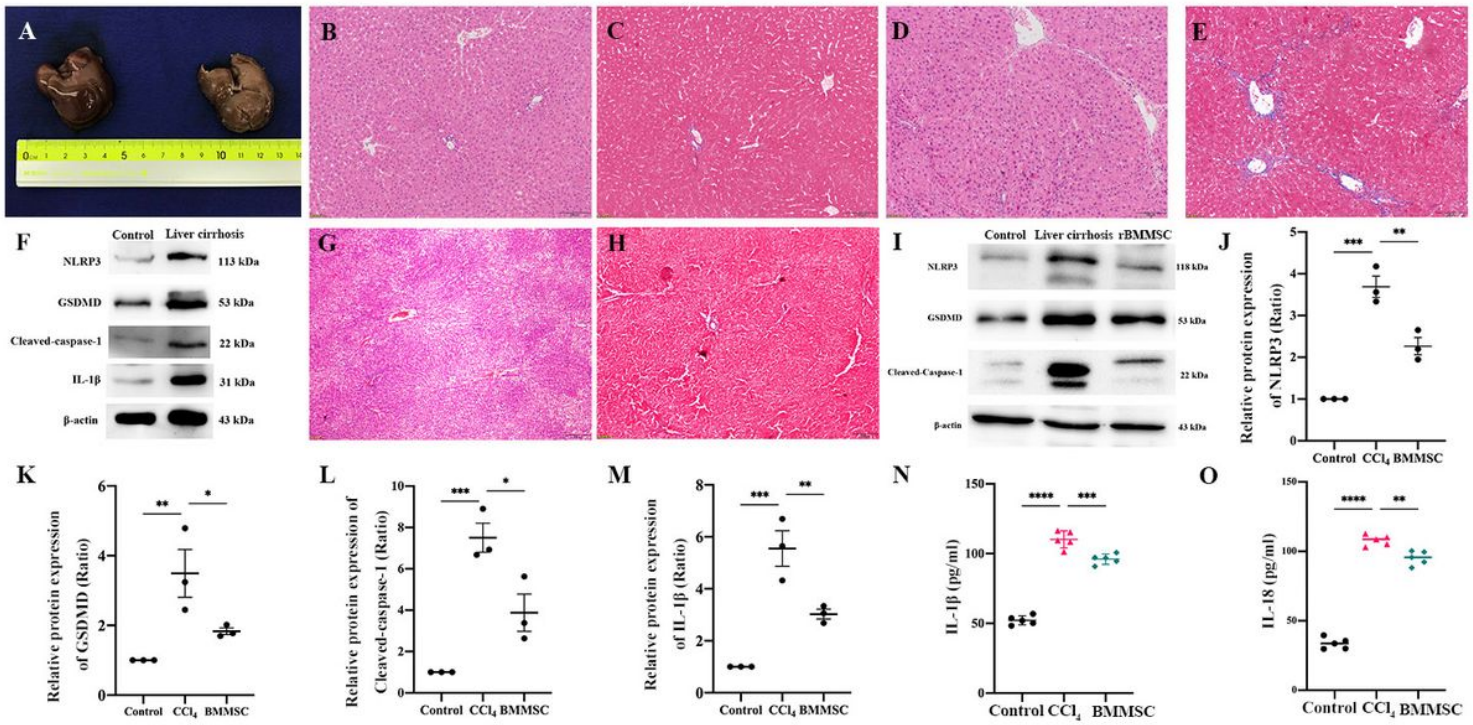

Figure 1

The alleviation of pyroptosis by rBMMSCs in the context of liver cirrhosis. Specimens of the control and cirrhotic liver models are shown in Fig. 1A. Pathological HE- and Masson-stained sections of control and cirrhotic liver tissues are shown (Fig. 1B-1E). Pyroptosis-related proteins were highly expressed in the liver cirrhosis model (Fig. 1F). Pathological sections showed significant alleviation in the rBMMSC transplantation group (Fig. 1G-1H). Pyroptosis-related proteins in the BMMSC group were significantly downregulated compared to those in the liver cirrhosis group (Fig. 1I-1M, *P<0.05 vs. the CCl4 group). IL-1β and IL-18 expression in the BMMSC group was dramatically decreased (Fig. 1N-1O, **P<0.01 vs. the CCl4 group). The data are displayed as the means ± SD.

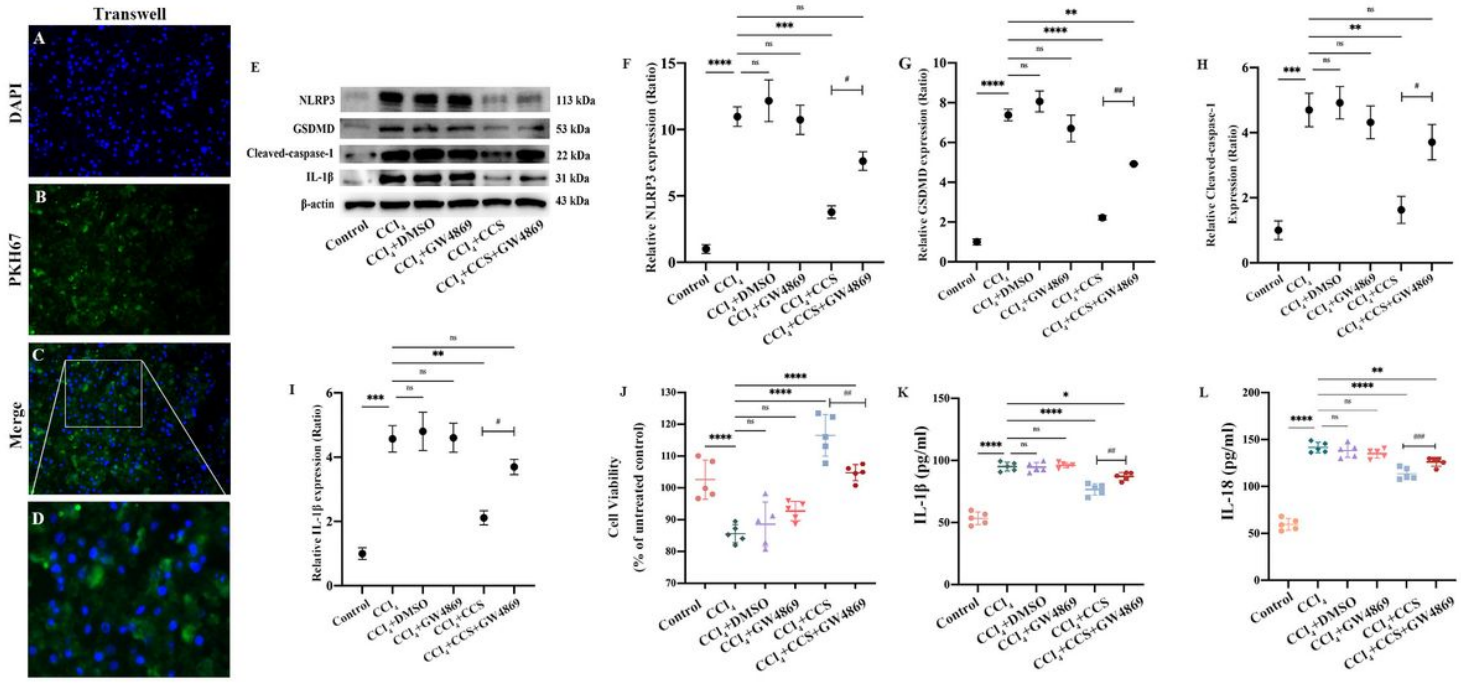

Figure 2

Paracrine effect by which rBMMSCs inhibit hepatocyte pyroptosis. PKH67 dye was transferred to hepatocytes by rBMMSCs via the paracrine pathway (Fig. 2A-2D). Pyroptosis-related proteins in the CCl4+CCS group were significantly decreased compared to those in the CCl4 group and CCl4+CCS+GW4869 group (Fig. 2E-2I, **P<0.01). The expression of pyroptosis-related proteins in the CCl4+DMSO and CCl4+GW4869 groups was not significantly different compared to that in the CCl4 group (Fig. 2E-2I). Cell viability in the CCl4+CCS group was significantly higher than that in the other groups (Fig. 2J, ##P<0.01). The expression of IL-1β and IL-18 in the CCl4+CCS group was dramatically lower than that in the other treatment groups (Fig. 2K-2L, **P<0.01). The data are displayed as the means ± SD.

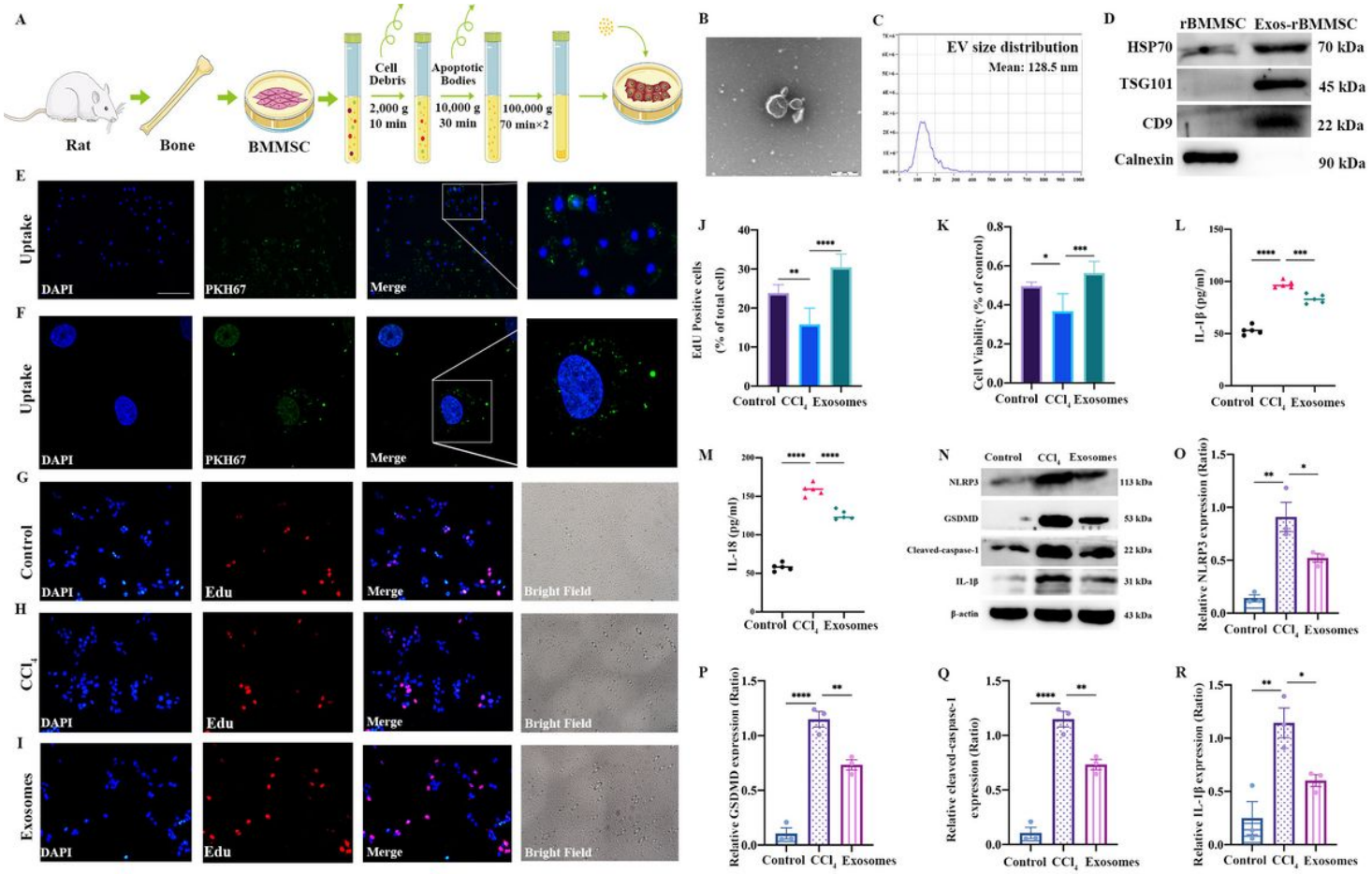

Figure 3

Effects of Exos-rBMMSC on CCl4-induced hepatocytes. The extraction protocol of Exos-rBMMSCs is shown (Fig. 3A). TEM morphology and nanoparticle tracking analysis (NTA) results are shown (Fig. 3B-3C). HSP70, TSG101, CD9 and calnexin expression in the rBMMSC and Exos-rBMMSC groups is shown (Fig. 3D). PKH67-labelled Exos-rBMMSC were internalized by hepatocytes, as observed under a fluorescence microscope (Fig. 3E-3F). Hepatocyte proliferation in the CCl4 group was dramatically increased (Fig. 3G-3K, ***P<0.001 vs. the CCl4 group). IL-1β and IL-18 expression in the Exo group was significantly decreased (Fig. 3L-3M, ***P<0.001 vs. the CCl4 group). NLRP3, GSDMD, cleaved caspase-1 and IL-1β expression in the Exo group was significantly decreased compared to that in the CCl4 group (Fig. 3N-3R, *P<0.05). The data are displayed as the means ± SD.

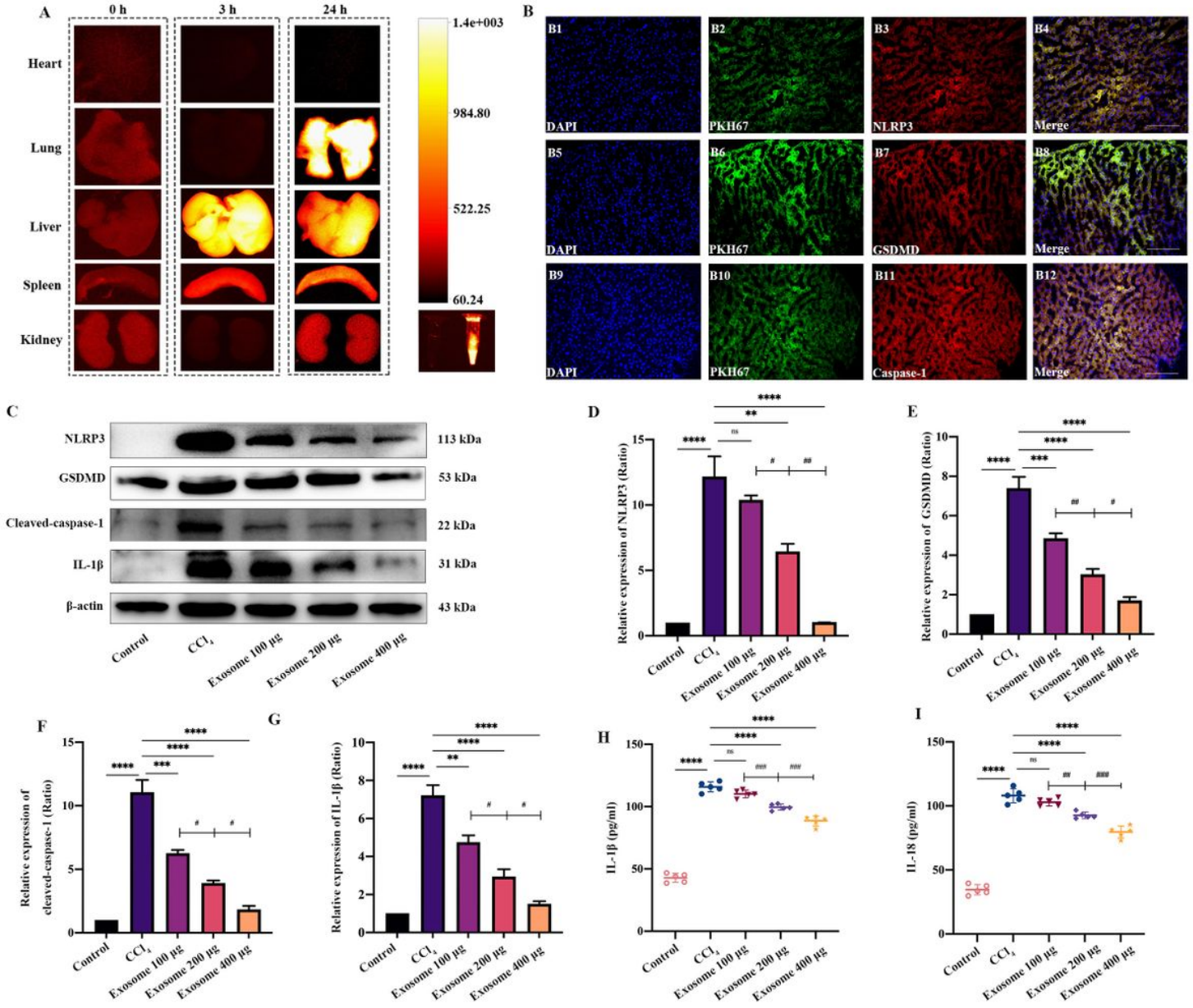

Figure 4

Distribution of Exos-rBMMSC and the therapeutic effect on liver cirrhosis. The distribution of Exos-rBMMSCs was examined by NIRF at 0 h, 3 h and 24 h postinjection. At 3 h postinjection, Exos-rBMMSC were mainly concentrated in the liver and were mainly concentrated in the liver and lung at 24 h postinjection (Fig. 4A). The colocalization of NLRP3, GSDMD and caspase-1 with PKH67 dye are shown in Fig. 4B. Compared to that in the CCl4 group, NLRP3, GSDMD, cleaved caspase-1, and IL-1β expression in the 200 μg and 400 μg Exos-rBMMSC groups was dramatically decreased (Fig. 4C-4G, **P<0.01). The expression of NLRP3 in the 100 μg Exos-rBMMSC group was not significantly different compared to that in the CCl4 group (Fig. 4D, P>0.05). The expression of GSDMD, cleaved caspase-1 and IL-1β in the 100 μg Exos-rBMMSC group was dramatically decreased compare to that in the CCl4 group (Fig. 4E-4G, **P<0.01). The expression of NLRP3, GSDMD, cleaved caspase-1 and IL-1β in the 200 μg Exos-rBMMSC group was significantly higher than that in the 400 μg Exos-rBMMSC group (Fig. 4C-4G, #P<0.05). IL-1β

and IL-18 expression in the 200 μg and 400 μg Exos-rBMMSC groups were dramatically lower than that in the CCl4 group (Fig. 4H-4I, ##P<0.001), while the expression in the 100 μg Exos-rBMMSC group was not different from that in the CCl4 group (Fig. 4H-4I, P>0.05). IL-1β and IL-18 expression in the 200 μg Exos-rBMMSC group were significantly lower than that in the 100 μg Exos-rBMMSC group but was higher than that in the 400 μg Exos-rBMMSC group (Fig. 4H-4I, ##P<0.01). The data are displayed as the means ± SD.

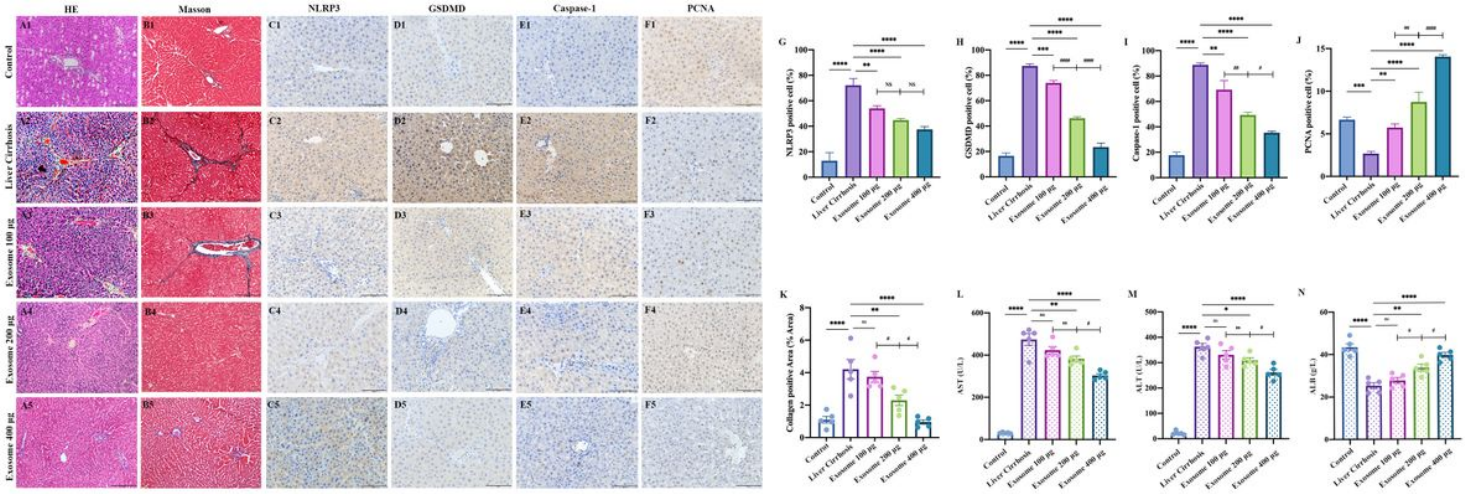

Figure 5

The therapeutic effect of Exos-BMMSC on liver cirrhosis was assessed in pathological sections and by measuring liver function. HE-stained sections from the control, liver cirrhosis and Exos-rBMMSC-treated groups are shown (Fig. 5A). Masson-stained sections from the different treatment groups are shown (Fig. 5B). Semiquantitative analysis of the collagen-positive area showed that the areas in the 200 μg and 400 μg Exos-rBMMSC groups were significantly decreased compared with those in the liver cirrhosis group (Fig. 5K, **P<0.01). The collagen area in the 200 μg Exos-rBMMSC group was significantly lower than that in the 100 μg Exos-rBMMSC group but was higher than that in the 400 μg Exos-rBMMSC group (Fig. 5K, #P<0.05). NLRP3-, GSDMD-, caspase-1- and PCNA-positive cells were assessed by immunohistochemistry (Fig. 5C-5F). Semiquantitative analysis showed that NLRP3-, GSDMD-, caspase-1- and PCNA-positive cells in the 100 μg, 200 μg and 400 μg Exos-rBMMSC groups were significantly lower than those in the liver cirrhosis group (Fig. 5G-5J, **P<0.01). The numbers of GSDMD-, caspase-1- and PCNA-positive cells in the 200 μg Exos-rBMMSC group were dramatically lower than those in the 100 μg Exos-rBMMSC group but were higher than those in the 400 μg Exos-rBMMSC group (Fig. 5G-5J, #P<0.05). NLRP3-positive cells in the 200 μg Exos-rBMMSC group were not significantly different from those in the 100 μg and 400 μg Exos-rBMMSC groups (Fig. 5G). AST and ALT expression in the 200 μg and 400 μg Exos-rBMMSC groups was significantly decreased, but ALB expression was significantly increased compared to that in the liver cirrhosis group (Fig. 5L-5N, *P<0.05). The expression of AST and ALT in the 400 μg Exos-rBMMSC group was dramatically lower, while the expression of ALB was higher than that in the 200 μg Exos-rBMMSC group (5L-5N, #P<0.05). The data are displayed as the means ± SD.

Supplementary Files

This is a list of supplementary files associated with this preprint. Click to download.

- Fig.6GraphicalAbstract.pdf